

1 **Testing sorption of uranium from seawater on waste biomass:** 2 **a feasibility study**

3

4 Steven McGowan¹, Hao Zhang², Claude Degueldre^{1*}5 ¹ Engineering Department, Lancaster University, Lancaster LA1 4YW, UK6 ² Lancaster Environmental Centre, Lancaster University, Lancaster LA1 4YW, UK

7

8 **Abstract**

9 The extraction of uranium from seawater has been successfully performed in batch mode on 15
10 selected biomaterials, including fruit, green vegetable and tuber samples. These biomaterial samples
11 were contacted in static batches with Irish seawater (2.8 ppb U) for periods of 1-2 months. After
12 sorption, both supernatants and HNO₃ digests from the sorbed biomass were analysed by inductively
13 coupled plasma mass spectroscopy (ICP-MS) for uranium.

14 Sorption of uranium from seawater onto the following materials revealed loadings ($\mu\text{g kg}^{-1}$) increases
15 from 10 to 20 for diced potato (*Solanum tuberosum*), Sultanas grape (*Vitis vinifera*), Brussels sprouts
16 (*Brassica oleracea*), and sweet potato (*Ipomoea batatas*), to 200-300 for skin of nectarine (*Prunus*
17 *Persica*), of orange (*Citrus Sinensis*) and of potato (*Solanum tuberosum*).

18 The fraction of sorbed uranium reached 92% to 98% for peanut shell, orange skin, Brussels sprouts,
19 garlic, grape pulp, grape skin, and Sultanas grape.

20 Consequently the K_d values were of the order of 50 to 200 mL g⁻¹ for mange tout (*Pisum sativum*),
21 sweet potato (*Ipomoea batatas*) whole, potato (*Solanum tuberosum*) whole, Brussels sprouts
22 (*Brassica oleracea*) and nectarine (*Prunus Persica*) skin, of 200 to 1000 mL g⁻¹ for grape (*Vitis*
23 *vitaceae*) pulp, Sultanas (*Vitis vinifera*) grape, peanut (*Arachis hypogaea*) shell, kale (*Brassica*
24 *oleriaceae*), lemon skin and grape (*Vitis vinifera*) skin, and finally of 1000 -2000 mL g⁻¹ for potato
25 (*Solanum tuberosum*) skin, orange (*Citrus Sinensis*) skin and garlic (*Allium sativum*).

26 Polyphenols are expected to increase sorption. The plot of K_d with polyphenol concentration displays
27 a positive correlation. Increases in sorption of may also be due to U(VI) reduction in U(IV) by

28 antioxidants reported on these biomaterials and by colloidal aggregation, suggesting irreversible
29 sorption.

30 This screening study aimed to select specific bio-waste material absorbents to be tested in detail in a
31 future study, prior tests at the pilot scale.

32

33 **Keywords:** uranium; seawater; extraction; biomass; sorption

34

35

36 *Corresponding author: Claude Degueldre, e-mail: c.degueldre@lancaster.ac.uk

37 **1. Introduction**

38

39 Nuclear power represents one of the cleanest energy vectors available to humans (Birol, 2019 [1])
40 partly due to the energy density of the fuel and partly due to the low mobility of the radioisotopes in
41 their waste form and the engineered environment, due to their strong sorption (Degueudre, *et al.*, 1994
42 [2] and 1996 [3]). With careful management, it is possible to ensure that all significant risks are
43 mitigated through engineering. In 1976, Pigford [4] stated:

44

45 *“The environmental acceptability of nuclear fission power plants rests upon the careful*
46 *control of environmental effluents from each of the many diverse steps in the nuclear fuel*
47 *cycle including uranium mining, fuel preparation, reactor operation, fuel reprocessing,*
48 *and the storage and disposal of radioactive wastes.”*

49

50 This is still fundamentally true today, as it was at the time. While the fuel cycle itself is under constant
51 review, economics have dictated that geological mining has continued to be the preferred route for
52 sourcing the uranium (U) necessary for the operation of a nuclear system at the current time (Ewing,
53 2004 [5]). However, uranium geological sources are finite, with some high-usage scenarios limiting
54 the supply of U to 80 years, with an estimated 7.6 Mt of U available at production costs of up to
55 \$260/kg of U extracted (NEA and IAEA, 2016 [6]).

56

57 A potential alternative exists, by extracting uranium from seawater. It is present at trace quantities
58 with an average of approximately 3.3 parts per billion (ppb or $\mu\text{g kg}^{-1}$) in standard seawater conditions
59 (35% salinity, pH 8.0), as a product of its annual input of approximately 10^4 tonnes by the rivers from

60 geological erosion, with approximately the same quantity being deposited (output) in deep sea
61 sediments. The total available in equilibrium at any time is 4500 Mt (e.g. Degueldre, *et al.*, 2019 [7]).
62 Research focussing on the use of man-made absorber has been prioritised since many years as
63 reviewed by Jun, *et al.*, 2022 [8].

64 There have been some attempts to extract this resource on test scales. The most successful was
65 attempted by a Japanese group, who placed braided chains of amidoxime-doped polyethylene into
66 deep-water conditions. Based on their experiment, they were estimated recovery of U at \$300 per kg,
67 assuming 20 reuses of the sorbing material (Sugo, *et al.*, 2001 [9]). This is considered the “Best
68 Possible Technology” existing so far for the application, but it remains uneconomic under current
69 market conditions (NEA and IAEA, 2016 [6]; Sugo, *et al.*, 2001 [9]; Schneider & Sachde, 2013 [10]).
70 Recently, Dong, *et al.*, 2019a [11], reported about the functionalization and fabrication of soluble
71 polymers of intrinsic microporosity for CO₂ transformation and uranium extraction. These are specific
72 microporous polymer PIM-1-based quaternary ammonium iodide. They were found to have the
73 highest uranium uptake ability tested in real seawater at pH 8.2 and room temperature for balanced
74 time of 10 to 4 h.

75 The same group also studied the enhanced uranium extraction by functionalization of cyano-bearing
76 conjugated porous polycarbazoles, see Dong, *et al.*, 2019b [12]. Cyano groups in polymers were
77 converted to conjugated polycarbazoles containing tetrazole or amidoxime groups after specific
78 treatment. In the real seawater with excess uranium, a maximum uranium extraction uptake of 119.4
79 mg g⁻¹ at room temperature was reported to be due to the strong chelating interaction between the
80 amidoxime groups and uranium.

81 More recently, Liu & Mao, 2021 [13] reviewed the potential of graphene oxide-based nano-materials
82 for uranium adsorptive uptake. Graphene oxide unique 2D structure, high specific surface area,

83 dispersion and hydrophilicity and abundant oxygen-containing functional groups provided excellent
84 adsorption potential for uranium extraction. In this review, the research status and progress of
85 graphene oxide-based nanomaterials for uranium adsorption were summarized. Their adsorption
86 capacities, influencing factors, kinetics, isotherms and thermodynamics were compared and
87 discussed. The microscopic mechanisms of uranium adsorption onto these absorbers were elaborated
88 at molecular level by spectral analysis, surface complexation models, and theoretical calculations.
89 The absorption models allow estimation of the sorption properties on the basis of physical and
90 chemical properties. The physical properties deal with the grain size, the fractal and/or the porosity.
91 As an example, Wei, *et al.*, 2018 [14] reported about sustainable cross-linked porous corn starch
92 adsorbents with high methyl violet adsorption. In this frame, and since smaller particles are stronger
93 than the larger one for their sorption potential, Song, *et al.*, 2019 [15] investigated the high adsorption
94 performance of methyl blue from aqueous solution using hyper-branched polyethyleneimine grafted
95 on short multiwalled carbon nanotubes as an adsorbent.

96

97 In a complementary way, Chen, *et al.*, 2019 [16], reported on the adsorption removal of pollutant
98 dyes, e.g. methylene blue, methylene orange and rhodamine B as model dyes, in wastewater by
99 nitrogen-doped porous carbons derived from pyrolysed natural leaves (*Euonymus Japonicus*).

100

101 In sorption, chemistry plays also a crucial role going from surface complexation with substitution
102 reactions as reviewed by Liu & Mao, 2021 [13] to the formation of specific compounds. This later
103 case was for example applied by Lin, *et al.*, 2019 [17] in their work on the efficient fluoride adsorption
104 in domestic water with reduced graphene oxide loaded silver nanomaterials.

105

106 Several recent studies extend the concepts.

107 Wang, *et al.*, 2020 [18] investigated hyperelastic magnetic reduced graphene oxide-aminated
108 nanomagnetite three-dimensional frameworks and reported their oil and organic solvent adsorption
109 capability.

110 Shi, *et al.*, 2021 [19] preparation of Mg,N-co-doped lignin adsorbents for enhanced selectivity and
111 high adsorption capacity of As(V) oxyanion from wastewater.

112 Hong, *et al.*, 2022 [20] proposed a highly efficient removal method for trace lead (II) absorption
113 and removal from wastewater using 1,4-dicarboxybenzene modified Fe/Co metal organic
114 nanosheets.

115

116 An alternative to the approach of using man-made absorber (e.g. plastics) would be to use a natural
117 material to sorb the uranium, which would not require specific absorbent synthesis. Many natural
118 materials include structures intended to selectively interact with elements in solution. These can be
119 either for functional, nutritional, or protective part of biological items. However, the original purpose
120 is actually irrelevant, if the relevant compounds can be extracted or otherwise exploited (Mata, *et al.*,
121 2009 [21]). This approach avoids utilisation of synthetic polymers as proposed in several projects
122 where weakness may be identified, such as lamination in amidoxime polymers assimilation or
123 covering with phytoplankton and assimilation by local fauna. In the coming years, it would be
124 expected that Governments first play an active role in addressing the issue of plastic waste by
125 introducing legislation to control all potential sources of plastic debris as proposed by Li, *et al.* (2016)
126 [22].

127

128 While these natural bio-sorbants are not as selective as the synthetic polymers, the lower production
129 costs, the strong sorbent properties for the elements of interest, and the high concentration effect from
130 the recovery process would potentially allow higher capacity on a per cost basis, compared with
131 materials that can cost 40% of the process as reported by Schneider & Sachde, 2013 [10].

132

133 The nature of these materials means they are often more prone to degradation of their sorption
134 capacity, in seawater conditions (although this is relatively minor under the timescales foreseen),
135 limiting reuse however they are selected for their lower costs that will mitigate the need to replace
136 them. As with the synthetic polymers, bio-fouling is likely to be the primary limiting factor in contact
137 time, as its growth is fuelled by the fraction of nutrients lost to solution from the biomass. This will
138 prevent further contact with the seawater, capping the influx (Park, *et al.*, 2016 [23]) although this is
139 known to be a capture process in its own right (Nakajima, *et al.*, 1982 [24]). The organisms produce
140 mucus as a pre-filter, which can precipitate toxic metals, including the elements of interest. Unlike
141 with the polymers, where the biofouling layer has to be removed to recover the elements of interest,
142 this layer is functionally indistinguishable from the materials, especially if suitably encapsulated.

143

144 While biomaterials has not been subject to a full scale attempt for the extraction of uranium from
145 seawater previously, some data is available from leach and tailing mining environments, where
146 attempts have been made to decontaminate ground or surface waters with a number of substances, or
147 aimed at elements other than uranium (Ramamoorthy, *et al.*, 1969 [25]; El-Sheikh, 2016 [26]; Tang,
148 *et al.*, 2013 [27]; Diallo, *et al.*, 2015 [28]; Gondhalekar & Shukla, 2014 [29]; Satari & Karimi, 2018
149 [30]). These tests are generally based on testing the sorption isotherm of the material, most commonly
150 in conjunction with a simulated liquid phase. The tested materials included *Myrica Cortex* barks

151 (Nakajima & Sakaguchi, 1989 [31]), *Citrus Limetta* peels (Gondhalekar & Shukla, 2014 [29]),
152 pyrolyzed tea and coffee wastes (Aly & Luca, 2013 [32]), Eucalyptus distillation sludge (Bhatti &
153 Hamid, 2013 [33]) and *Citrus* reprocessing wastes (Satari & Karimi, 2018 [19]; Pathak, *et al.*, 2015
154 [34]). In addition specific biological substances, such as chitin and chitosan, were tested as received
155 (Sakaguchi, *et al.*, 1979 [35]) or treated (Sakaguchi, *et al.*, 1981 [36]). Rather than testing materials
156 one at a time, with inconsistent methodology, tests were performed utilizing these materials on a
157 standardised approach, using natural seawater, rather than the historical approaches involving
158 simulated seawater mentioned above.

159

160 In addition to the material properties, it is important to not lose sight of the key benefit of these
161 materials: the low cost. In practice, this has proved to be hard to quantify, as there is no marketplace
162 for many. As a general rule, by-products of food crops such peels or husks, **are** preferential as their
163 supply generally outstrips demand: their “price” is only the transport and processing costs, which is
164 outside the scope of this work. Therefore, the materials of interest are by-product, or otherwise low
165 cost biomaterials, which can be dried effectively, with high surface area and antioxidant compounds.

166

167 Biomass has also been used in other fields that sorption. As an example, Xie, *et al.*, 2018 [37],
168 reviewed the applications of unmodified and modified cellulose nanocrystals in papermaking
169 industry, reinforcing filler for polymers, shape memory polymers, healable polymeric materials, food
170 industry, drug carrier in pharmaceutical industry, supporting matrix for catalysts, and nano-medicine.
171 Cai, *et al.*, 2019 [38] proposed a robust construction of flexible bacterial cellulose paper for high
172 capacitance and sensitive sensors for H₂O₂ detection. Yuan, *et al.*, 2020 [39] reported and reviewed
173 about nano-cellulose-based composite materials for wastewater treatment and waste-oil remediation.

174 Boni, *et al.*, 2020 [40] combined silk sericin, known for its antioxidant and mitogenic effects, with
 175 surface micro-patterns in bacterial cellulose dressings to control fibrosis and enhance wound healing.
 176 More recently, Mu, *et al.*, 2021 [41] proposed a high value utilization of bio-oil from lignin targeting
 177 for advanced lubrication.

178 This study is part of an attempt to develop a new nuclear fuel cycle, including uranium extraction
 179 from seawater, and its utilization in a fast molten salt reactor, in order to develop a renewable nuclear
 180 fuel cycle as described recently in Degueldre, *et al.*, 2019 [7].

181

182

183

2. Sorption background

184

185

186

187

188

189

190

191

192

Sorption is traditionally described by reactions between specific groups and the metal or complex ions (Degueldre, *et al.*, 1994 [2]; Joseph, Van Loon *et al.*, 2013 [42]). Considering a generic surface $>Su$, above a macromolecule, substrate or colloid (\diamond), associated with one or more exposed ‘hydroxyl’ groups $\diamond>Su(OH)_n$. They are in contact with an aqueous phase with which specific chemical exchanges may take place. Typically, for biomaterials, these groups could be phenolic or carboxylic.

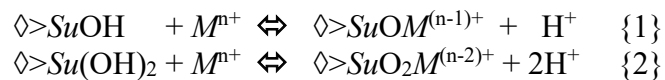
A metal ion M^{n+} or their complexes ($M(OH)_i^{(n-i)+}$) may complex to the surface, by substitution with one or more of the protons.

193

194

195

196



197

These reactions may result in a bond which may be of variable strength (Degueldre, *et al.*, 1994 [2]).

198

There are three factors that control how strong surface complexation is and how likely that this

199

reaction is to be reversible.

200

- 201 1) The species of **ions or complexes** in solution dictate the strength of surface
202 complexation on a site. To estimate their surface complexation constant values
203 correlations with the hydrolysis constants are used. These values which are readily
204 available for a large body of ions and complexes and can be extended by correlation
205 to others (Degueldre, *et al.*, 1994 [2]; Degueldre, *et al.*, 2001 [43]).
- 206 2) The **active groups at the surface** of the sorbing material have an effect on the surface
207 complexation of the bond. These structures can be classified into groups of
208 compounds with similar mechanisms, but different morphologies. The two common
209 examples in bioorganic systems are carboxylic and phenolic groups.
- 210 3) The relative **concentration of these species** in solution and the **pH** play a relevant
211 role in the surface complexation process starting with the strongest (poly-dentate) to
212 the weakest (mono-dentate).

213 The sorption is traditionally described on the basis of the concentration of metal sorbed on the solid
214 $[M]_s$, and the dissolved metal in the fluid (water) phase $[M]_w$ or $[M]_l$ depending on the unit basis.

215

216 For dynamic systems, it is possible to quantify sorption using the sorbed fraction F (%) as defined in
217 Eq. (1) below.

218

$$219 \quad F = 100 \frac{[M]_s}{([M]_s + [M]_l)} \quad (1)$$

220

221 Where $[M]_s$ and $[M]_l$ are in $\mu\text{g kg}^{-1}$. Note that this is primarily a “living” ratio, and may be calculated
222 even if the system is not at equilibrium.

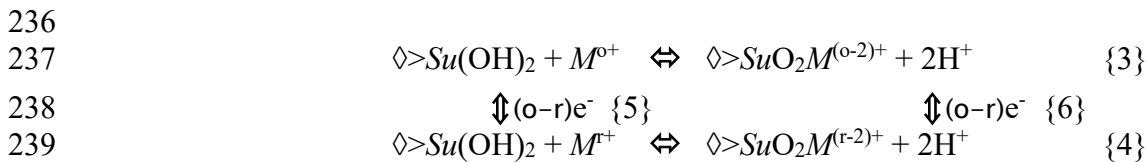
223

224 A more formal way to quantify this ratio is the sorption constant K_d , as defined by Eq. (2) for reactions
 225 {1} & {2} at equilibrium:

$$226 \quad K_d = [M]_s/[M]_w \quad (2)$$

227
 228 With $[M]_s$ the concentration of all metal species on the surface of the absorbent (g g^{-1}) and $[M]_w$ the
 229 concentration of all metal species in solution (g mL^{-1}). The K_d values are then given in mL g^{-1} (or L
 230 kg^{-1}).
 231

232 For redox sensitive species, in addition to the direct sorption process occurring for a given redox state,
 233 there are indirectly redox effects, as different forms of complexes and ions (oxidative and reductive)
 234 have different hydrolysis constants, so have different sorption properties. The reactions at the surface
 235 and in the area of effect form a cycle that can be generalised to {3} - {6}:



239
 240 This concept of K_d can be applied and a net Eq. (2) can be adapted for all species at the surface and
 241 in solution. For example, if the direct effect of sorption described by reaction {4} produces stronger
 242 sorbed species than {3} then the reduction of the metal by {6} will control the sorption by {4} to a
 243 greater degree than {3}. The net result would be the sorption of the oxidative species may generate
 244 the reductive complexes at the surface, due to a reduction of the sorbed species after fixation.
 245
 246

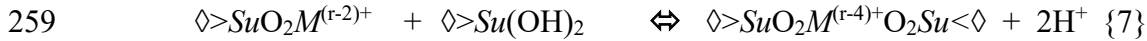
247 For the specific example of U, as the focus of this study, the ion can exist under several oxidative
 248 states. In surface waters, U is normally hexavalent. Its sorption in neutral conditions is strong, but
 249 when reduced as tetravalent U it exhibits even stronger sorption. This is considered to be due to a
 250 Coulomb effect, as the binding for U^{4+} complexes is known to be stronger than for the UO_2^{2+}

251 complexes (McKee & Todd, 1993 [44]). Therefore, a reducing agent e.g. antioxidants from the
 252 biomass material, introduced into solution, will increase the proportion of U^{4+} present, and increase
 253 the effective K_d values for U.

254

255 These sorbed species still have an interactive potential for further reactions with species in solution,
 256 which means they have become a reactive surface. This is a factor for both free species, and other
 257 surfaces. For example, in these circumstances, colloidal materials can interact as per {7}:

258



260

261 Clearly in this case the $\diamond>SuO_2M^{(r-4)+}O_2Su<\diamond$ structure will not allow the ions $M^{(r-4)+}$ (which may be
 262 a complex of the form $M(OH)_i^{(r-i)+}$) to return to the aqueous phase. They are quenched in the
 263 macromolecular phase of the colloid aggregate and are fixed on it with only extremely low possibility
 264 of desorption. In this case, the sorption becomes effectively irreversible and the K_d becomes a plain
 265 sorption ratio, leading to very high effective K_d values.

266

267 An additional factor to this model is, in practice, natural sorbents are not exclusively one sorbing site
 268 type, and exist on a sliding scale, between wholly polyphenolic, and wholly carboxylic
 269 polysaccharides. However, both materials are based on a similar sized replicating unit for lignin or
 270 hesperidin in polyphenolic compounds, and cellulose or demi-cellulose for polysaccharide, due to the
 271 mechanical processes in synthesis in biomaterials (Boudet, 2000 [45]). This has the consequence that
 272 it is only necessary to measure the proportion of the relevant structures to be able to estimate the
 273 material composition net (direct effect) K_d . Further to this, it is necessary to consider that certain
 274 compounds and classes of compounds are known to be high in antioxidants: for example, tannins are
 275 a class of compounds with antioxidant properties present in many plant species, due to their use in

276 transport and defence mechanisms. As a polyphenolic compound, these also function as a sorption
277 site, and some are known to actively co-chelate to form insoluble compounds with metal ions,
278 permanently removing from solution (Zhang, *et al.*, 2016 [46]).

279

280 For the purposes of maximising the effective surface area of sorbent, if it is finely dispersed, the
281 processes would favour the aggregation, making sorption of U irreversible on specific biomaterial.
282 Therefore, these materials are to be investigated to find the optimum performance for the extraction
283 of U.

284

285

286

287

3. Experimental

288 In order to calculate the sorption constant K_d , it is necessary to measure the concentration of the metal
289 in solution and at the biomaterial surface, at equilibrium. The following section deals with the water
290 sampling, selection and preparation of biomass materials, and the methodology of analysis.

291

3.1 Materials selected for sorption tests

292

293

294

3.1.1 Water Samples

295

296

297

298

299

300

301

302

For the purposes of supplying seawater, 3 batches of 2.5 L water samples were collected from
Trafalgar Point (54.075192 N, -2.878758 W), Stone Jetty, Morecambe, NW UK, on the Irish Sea (see
Fig.1), at high tide, at 09:33am on the 19 of January 2019; at 10:38am on the 15 of June 2019 and at
07:32am on the 15 of August 2019. These water salinities (around 3.2%, per Jones (1991) [47]
corresponding to 91% dilution and 1.023 g mL^{-1} density) are known to be slightly below the salinity
the average seawater (3.5%) found on Earth because of some local mixing with estuary water.
However, since these surface seawater samples were collected on non-rainy days over the Morecambe

303 Bay area, these samples can be considered to be a good representative for the composition found in
304 Irish seawaters.

305
306 **Fig. 1:** Map of the Irish Sea 50-56°N, 2-8°W, and of Morecambe 54°N, 3°W, sampling point ●
307

308

309

310 **3.1.2 Biomass Samples**

311

312 All biomass materials are vegetal and sourced through suppliers within Lancaster.

313 To represent fruits, **orange skin** (*Citrus Sinensis*), **lemon skin** (*Citrus Limon*) and **nectarine skin**
314 (*Prunus Persica*) were selected as readily available material which are commonly discarded. These
315 have a large volume produced through industrial processing, mainly consisting of the skin, which is
316 currently used for animal fodder, although some use for the production of flavourings are also
317 common. These fruits are all known to have high polyphenolic compound concentrations for fruits,
318 particularly in the skins, where they serve important biological functions. To prepare the samples,
319 they were dried, and the pith on the oranges and limes was removed, as far as practical. They were
320 then diced so not to exceed 4 mm on any axis.

321

322 **Grapes** (*Vitis*) have extensive and specific regions dedicated to their harvest, for the purposes of wine
323 production. These have a large volume of solid by-products, mainly consisting of the skin, which is
324 currently mainly used for animal fodder. Grapes are associated with well-studied antioxidant
325 chemicals e.g. tannin, and are known to be easily dried and powdered for the purposes of the present
326 study. Given the range of species and cultivation purposes, two variants were selected as
327 representatives.

328

329 A **red grape** (*Vitis vitaceae*) was selected, as reasonable middle ground of grape varieties. One
330 subsample was pulped whole, while a second had the skin separated, to measure its specific effect.
331 Furthermore, **sultanas grape** (*Vitis vinifera*), which are a variety of white grape that has been dried
332 to raisin standards, were selected as an easily available grape material that had underwent commercial
333 drying. As skinning was not practical, the samples were split into one subsample of whole sultanas,
334 and one subsample minced through a 4 mm diameter grate, to compare exterior surface to internal
335 bulk properties. This had limited effect, due to particle cohesion.

336

337 **Kale** (*Brassica oleriaceae*, var. *Acephala*), **mange tout** (*Pisum sativum*, var. *macrocarpon*), **garlic**
338 (*Allium sativum*) and **Brussels sprouts** (*Brassica oleracea*) were selected to represent a number of
339 useful species that are otherwise difficult to source as a by-product. Kale is known to be high in
340 antioxidant properties, stemming from both polyphenolic compounds, and sulphur-rich compounds,
341 and has a high surface area. Brussels sprouts are similar, but have much higher proportion of sulphur-
342 rich compounds compared to the polyphenolics present in kale. Garlic contains several chelating acids
343 known to precipitate heavy metals. Mange tout is high in a number of antioxidants, particularly
344 retinoic acid, which have important scavenging effects in biological systems.

345

346 Ground vegetable tubers have been known to sorb heavy metals from their surrounding soil, during
347 their normal life processes. These are filtered and concentrated utilizing their skin, so a **white potato**
348 (*Solanum tuberosum*) and a **sweet potato** (*Ipomoea batatas*) variety were selected. As with the grapes,
349 each were split into two subsamples, one where the skin was separated, and one where they were
350 diced through a 4 mm diameter grate.

351

352 Another option is the common by-product of **Peanut** (*Arachis hypogaea*) products, where the shells
 353 are removed. These have a wide but weak use in a variety of industries, such as fibre production and
 354 in construction, but the most common disposal route is by incineration, either, for direct disposal or
 355 converted to smokeless fuel for domestic heating. These are known to have high site capacity, and
 356 fixed polyphenolic compounds suitable for heavy metal sorption, and have been used in remediation
 357 techniques, as a natural sorbent for some heavy metals. As with the previous materials, they were cut
 358 into 4 mm diameter squares.

359 As previously described, samples of the bio-materials were cleaned, chopped and separated. The
 360 samples that were not already sized were cut into 4 mm² segments. A small subsample of each
 361 (displayed in Table 1) was separated, weighed, and dried using an Aicok© Digital Dehydrator, at
 362 50°C for 72 hours (Under N₂). It was then weighed (precision 1 mg), to establish the dry weight
 363 conversion factor. This was used to adjust the mass values in Table 1 to dry basis.

364

Table 1: Dry weight conversion

Sample	Wet Mass (g)	Dry Mass (g)	Water Lost (g)	Water fraction %
Orange skin	28.39	8.67	19.72	69.4%
Lemon skin	22.60	4.35	18.24	80.7%
Nectarine skin	23.86	3.51	20.36	85.3%
Grape skin	15.11	2.95	12.16	80.5%
Grape pulp	109.00	45.69	63.31	58.1%
Sultanas whole	99.14	23.75	75.39	76.0%
Brussels sprouts	55.89	10.92	44.98	80.5%

Kale diced	14.92	2.17	12.75	85.4%
Mange tout	32.43	5.41	27.03	83.3%
Garlic diced	9.28	0.38	8.90	95.9%
Peanut shell	1.87	1.74	0.13	6.9%
Potato skin	2.23	0.47	1.75	78.8%
Potato whole	14.51	3.57	10.94	75.4%
Sweet potato whole	23.73	5.70	18.03	76.0%

365

366

367

368 **3.2 Batch methodology**

369

370 Where mentioned, deionised water is Suprapure© Quality. A 100 mL and 500 mL volumetric flask
371 is approximately half filled with deionised water, and labelled appropriately. In a fume cupboard, 64
372 mL of concentrated nitric acid (Aldrich© 70% redistilled, $\geq 99.999\%$ pure) is slowly pipetted into the
373 100 mL volumetric flask, shaking regularly to fully disperse the acid and heat. Vial is then slowly
374 made up to the mark with deionised water and shaken to ensure full dispersal. The 100 mL flask is
375 then slowly added to the 500 mL flask, rinsing regularly to ensure complete transfer and is made up
376 to the mark, and mixed. The final solution is transferred to a storage bottle. This was repeated 4 times
377 over the course of the work. This solution is referred to as the 2 M nitric solution.

378

379 With organic material, in practice it is difficult to establish that a formal equilibrium has been reached,
380 due to the dynamic nature of the materials. As the material undergoes fragmentation, more surfaces

381 are exposed, increasing the number of available sites, while existing sites may, in turn, be permanently
382 deactivated and become non-functional. Therefore it is expected that the K_d will exist on a curve,
383 which will change over time, which must be actively tested, to allow prediction.

384

385 While fragmentation is occurring, the structural materials have longer dispersal rates, which are low
386 enough that this would not be a concern. However, to contextualise this process, the liquid phase
387 sampling process was designed with the intention to allow measurement of fractionalisation
388 between these fragments which were larger than 0.4 μm , and the liquid phase. If this fraction proved
389 significant, then it would be possible to enclose the material in a boundary layer (a filter bag), which
390 would prevent further transport outside the system. However, these sub 0.4 μm phase samples
391 proved to be prone to micro-organism growth and were unable to be analysed.

392

393 Samples were prepared in Corning™ 50mL Plug seal cap polypropylene self-standing centrifuge
394 tubes. These were labelled, and pre-weighed, to establish the zero weight of the sample. Batch
395 component masses and ratio at contact time are given in Table 2.

396

397

398

399

Table 2: Batch component masses and ratio at initial contact time.

Sample	Sample1. Biomass (g)	Sample 1. Seawater mass (g)	Ratio	Sample2. Biomass (g)	Sample 2. Seawater mass (g)	Ratio	Contact Time
Orange skin	0.177	25.41	0.007	0.281	25.58	0.011	2 months
Lemon skin	0.349	25.40	0.014	0.222	25.19	0.009	2 months
Nectarine skin	0.132	26.04	0.005	0.207	25.16	0.008	2 months
Grape skin	1.061	25.44	0.042	0.946	25.65	0.037	2 months
Grape pulp	3.800	25.06	0.152	6.800	25.52	0.266	2 months
Sultanas whole	5.680	25.45	0.223	5.010	25.59	0.196	2 months
Sultanas diced	5.480	25.28	0.217	5.480	25.44	0.215	2 months
Brussels sprouts	3.680	25.55	0.144	4.770	25.51	0.187	2 months
Kale diced				0.428	25.41	0.017	2 months
Mange tout	0.804	40.64	0.020	1.002	38.91	0.026	1 month
Garlic diced	0.673	40.11	0.017	1.744	39.07	0.045	1 month
Peanut shell	1.337	43.63	0.031	0.804	45.64	0.018	1 month
Potato skin	0.199	44.64	0.004	0.165	50.86	0.003	1 month
Potato whole	3.364	32.02	0.105	3.084	34.52	0.089	1 month
Sweet potato whole	2.061	36.12	0.057	2.293	36.52	0.063	1 month

400

401

As previously described, samples of the bio-materials were cleaned, chopped and separated. The

402

samples that were not already sized were cut into 4 mm² segments. A small subsample of each

403 (approximately 5 g) was separated, weighed, and dried using an Aicok© Digital Dehydrator, at 40°C
404 for 72 hours. It was then weighed, to establish the dry weight conversion factor.

405

406 Two replicated subsamples of each of the materials of was placed into the sample vials, and the weight
407 recorded. Then the volume was made up to 40 mL, and the weight of water added is recorded. These
408 samples were left undisturbed for at least one month to equilibrate.

409

410 A third sample of each of the biomaterials was separated and left without contact with the seawater,
411 in order to establish ground state concentrations of the materials.

412

413 Further to this, samples of the seawater were placed into sample tubes, without any biomass present,
414 to act as system controls, to establish if there were any losses in processing.

415

416 At the end of the leave time, the samples which had seawater present were partitioned.

417

418 A volume of 10 mL of the aqueous phase was extracted using a mechanical pipette and digested in
419 10 mL of heated 2 M HNO₃. The remainder was then filtered using a Whatman™ 0.4 µm PTFE
420 membrane filter, then made up to 100 mL, using a clean volumetric flask. The solution was then
421 transferred to a clean tube for storage.

422

423 In parallel to this, the remainder was filtered using a Whatman™ 595 150 mm filter paper to capture
424 the solids, then they were digested in 20 mL of heated 2 M HNO₃, then filtered through a Whatman™
425 0.4 µm PTFE membrane filter then made up to 100 mL, using a clean volumetric flask. The solution

426 was then transferred to a clean tube for storage. In addition to the samples themselves, the blank and
427 control samples were also subjected to the same process.

428

429 All samples were then diluted by a factor of x20 with deionised water, to minimise the impact of salt
430 precipitation on the ICP-MS instrumentation.

431

432 **3.3 Sample analysis**

433 **3.3.1 Biomass sample characterisation**

434

435 A subset of samples was identified as of particular interest, and were selected for analysis by
436 Fourier Transform Infrared (FTIR) spectroscopy. These were the dried kale diced sample, garlic
437 powder, grape skin, orange peel, peanut shell and potato skin. Spectra were also recorded on the
438 dried sorbed samples after contact with seawater and phase drying as described above for each
439 sample which was dried using the same protocol as for the initial samples. Together with a control
440 sample of each, they were analysed by a Shimadzu IRTracer-100 with attenuated total reflection
441 (ATR) stage, in the UTGARD facility at the Engineering Department, Lancaster University.
442 Analysis was by absorbance of the total reflection using Happ-Genzel apodization. The spectral
443 resolution was 1 cm^{-1} , over the range $600 - 4000\text{ cm}^{-1}$ and for 45 scans. Samples were analysed on
444 the basis of a consistent volume, as they are intended for only comparative review to assess
445 alteration.

446

447

448 **3.3.2 ICP-MS analysis**

449

450 Samples were analysed by ICP-MS at Lancaster Environmental Centre Trace Metals laboratory using
451 a Thermo Fisher Scientific Series X7. The ICP-MS spectrometer is installed in a dust free laboratory
452 equipped to avoid contamination.

453

454 Because of interference with the salt, which is typically 35 g kg^{-1} , a dilution by a factor of 20 is
455 required to record artefact free readings because of crystallisation on the cone. The injection rate was
456 0.3 mL per time unit (10 seconds). The dwell time for uranium was 10 ms .

457

458 In this bulk of this work, the difference between an experimental and average value is referred to as
459 the absolute error, which for paired samples would be equivalent to the Standard Deviation (SD).

460 Otherwise, where the sampling involved multiple results, the formal definition of Standard Deviation
461 was applied. When the absolute error is divided by the mean value it becomes the relative error, or
462 the relative standard deviation, as appropriate. Percent error is relative standard deviation (RSD)
463 multiplied by 100%.

464

465

466 **4 Results**467 **4.1 Biomass sample analysis**

468 Samples were analysed by FTIR on the basis of a consistent volume, as they are intended for only
469 comparative review to assess alteration and compare the density of active groups from one sample to
470 others. It was observed that the control samples were more homogeneous in size, as the contact
471 samples had partially clumped, forming during the redrying process loosely cemented
472 conglomerations of finer particles. This was mostly visible in orange peel, peanut shell and grape
473 skin, while the others were more consistent.

474

475 In most cases, the two samples have no variation in location of the peaks, only intensity, with the post
476 contact samples generally being less intense than the pre contact samples. This can be attributed to a
477 shielding effect from salt crystals, and the larger particle size (and hence lower surface area). This is
478 illustrated by two samples which do not follow this pattern (garlic and kale) which experienced the
479 highest fragmentation of the samples, and so the variation in intensity can be attributed to increased
480 surface area through the contact period.

481

482 As would be expected, given the material's organic nature, the signals are dominated by those
483 associated with cellulose. Peaks at $\sim 3300\text{ cm}^{-1}$ (O-H), 1200 cm^{-1} (C-H₂) and 1050 cm^{-1} (C-O and C-
484 C) are all clearly visible and are broadly similar between samples. Of interest as potential sites for
485 sorption, in most cases, at least a single (merged) peak, or a double peak associated with carboxylic
486 groups are visible at $1720\text{-}1620\text{ cm}^{-1}$ are clearly present in all samples, and a region of activity which
487 would correspond with a double peak associated with polyphenolic groups is visible at $1400\text{-}1200$

488 cm^{-1} . The IR spectra recorded for the prior and post contacted samples with natural seawater are
489 given in Fig. 2.

490

491 Post contacted grape skin has the notable exceptional feature of the carboxylic double peak at 1720-
492 1620 cm^{-1} being more intense than pre contact, which can be attributed to either an increase in
493 sorbance sites through specific processes, or the sorbance effects leaving them more exposed to be
494 sensed by the FTIR.

495

496 Although kale diced exhibits much greater activity due to dispersal, one feature of a double peak at -
497 $2900\text{-}2800 \text{ cm}^{-1}$ stands out as quite distinct: a C-H bond under stretched and aldehydic conditions
498 respectively. This is probably a fermentation effect.

499

500 Garlic would be the normal response of the dispersing material. The increased response on each of
501 the peaks is fairly consistent in proportion between the peaks.

502

503 Orange peel, peanut shell and potato skin are the three samples which exhibit consistent but reduced
504 peak pattern between the samples. The notable exceptional features are potato skin having a higher
505 carboxylic double peak, and peanut shell exhibiting reduced carboxylic peak, compared to their pre-
506 contact baseline.

507

508 **Fig 2.** IR spectra of the samples prior and post contact with natural seawater.
509 Samples: A grape skin, B kale diced, C garlic, D peanut shell, E potato skin, F orange peel.

510

511

512 **4.2 Uranium analysis in standard**

513

514 A mass scan range was first set for standardisation. It ranged from 45 (scandium), 103 (rhodium), 208
515 (lead) or 209 (bismuth) and 238 (uranium).

516 For uranium calibration, uranium solutions of 0.1, 0.3, 0.6 and 1.0 $\mu\text{g L}^{-1}$ were prepared from a
517 reference standard uranium solution (sourced from VWR), together with a zero standard of ultrapure
518 water were analysed for a calibration curve. In addition, a broadband reference standard was added
519 for traceability. The calibration curve proved to be linear (see Fig. 3) over this range ($R^2 = 0.9948$),
520 with an increasing variance from 1.0 - 4.6%. Most of this variance is instrumental in nature: samples
521 experience a small dilution effect between the first sampling and the following ones. The noise factor
522 of the system was measured from the 0 standards, resulting in a zero variance of 8.62 counts,
523 corresponding to a concentration of 0.000127 $\mu\text{g L}^{-1}$. Therefore, the 3- σ value (Degueldre, 2017 [48])
524 for as the limit of detection is 0.0004 $\mu\text{g L}^{-1}$ (ppb) or 0.4 ppt.

525

526 **Fig 3:** ICP-MS calibration curve for uranium.
527 Conditions: injection rate: 0.03 mL s^{-1} ; dwell time 10 ms.

528

529

530 **4.3 Analysis of uranium in seawater samples**

531

532 The seawater samples were gathered on 3 separate campaigns. These were analysed and were
533 considered similar enough between the sampling times as to not have an appreciable effect on the
534 results (see Table 3). The average value of $2.69 \pm 0.41 \mu\text{g L}^{-1}$ is below (82%) that conventionally
535 ascribed to the sea ($3.3 \mu\text{g L}^{-1}$, 100%) (Diallo, *et al.*, 2015 [28]). However, this is likely due to
536 sampling being near-shore, which is due to a small dilution factor (e.g. 91% see Section 3.1.1) due to
537 freshwater runoff (Laane, *et al.*, 1996 [49]), and a weak scavenging effect from phosphates, which
538 are known precipitants for uranium (Beazley, *et al.*, 2007 [50]).

539

540
541 **Table 3:** Uranium concentration in seawater as sampled for this study

Uranium concentration ($\mu\text{g L}^{-1}$)	Sample 1 09:33 am, 19-01-19	Sample 2 10:38 am, 15-06-19	Sample 3 07:32 am, 15/08/19	Average
	2.27	2.29	2.48	
	± 0.07	± 0.02	± 0.00	
	2.89	2.66	3.53	
	± 0.16	± 0.29	± 0.17	
		2.92	3.21	
		± 0.03	± 0.03	
		2.32	2.35	
		± 0.31	± 0.38	
Average	2.58	2.55	2.89	2.69
RSD	12.10%	10.21%	17.00%	15.33%

542
543
544 There are several isobaric interferences that can be anticipated to impact on the accuracy of the ICP-
545 MS measurements of uranium ^{238}U in seawater.

546 The only single isotope interference would be due to $^{238}\text{Pu}^+$. However, plutonium is nearly absent in
547 seawater today ($\ll \text{fg L}^{-1}$).

548 There are however, several cluster ions which could potentially impact readings. Heavy metal cluster
549 ions where there is an attachment with O, C, Ar, Cl and H isotopes, which would all be present at
550 significant concentrations. The most likely are the following cluster ions, which are given below,
551 alone with their elemental concentration in seawater. From these, we can conclude that none of these
552 cluster ions would significantly interfere with ^{238}U because the concentrations of their heavy element
553 cluster ions are several order of magnitude below that of uranium in seawater.

554

555 • $[\text{}^{222}\text{Rn}^{16}\text{O}]^+$, with a maximum potential concentration of $6 \times 10^{-19} \text{ g L}^{-1} \text{ Rn}$ (Gregoriè, *et al.*, 2008

556 [51])

- 557 • $[^{226}\text{Ra}^{12}\text{C}]^+$, with a maximum potential concentration of $\sim 9.8 \times 10^{-14} \text{ g L}^{-1}$ Ra (Walker & Rose,
558 1990 [52])
- 559 • $[^{198}\text{Hg}^{40}\text{Ar}]^+$ with a maximum potential concentration of 9.97% of $5 \times 10^{-9} \text{ g L}^{-1}$ Hg (Gardner,
560 1973 [53])
- 561 • $[^{202}\text{Hg}^{36}\text{Ar}]^+$ with a maximum potential concentration of 29.86% of $5 \times 10^{-9} \text{ g L}^{-1}$ Hg and 0.337%
562 Ar (Gardner 1973 [53])
- 563 • $[^{237}\text{Np}^1\text{H}]^+$ with a maximum potential concentration of $<10^{-12} \text{ g L}^{-1}$ Np (Assinder, 1999 [54])
- 564 • $[^{198}\text{Pt}^{40}\text{Ar}]^+$ with a maximum potential concentration of 7.2% of $<10^{-12} \text{ g L}^{-1}$ Pt (Turetta, *et al.*,
565 2003 [55] & Goldberg, *et al.*, 1986 [56]) .
- 566 • $[^{201}\text{Hg}^{37}\text{Cl}]^+$ with a maximum potential concentration of 13.18 % of $<5 \times 10^{-9} \text{ g L}^{-1}$ Hg, and
567 24.23% Cl (Gardner 1973 [53]).

568

569 However, none of these cluster ions interfere with ^{238}U because the concentration their heavy
570 element cluster ions is several order of magnitude below that of uranium in seawater.

571

572 **4.4 Analysis of supernatants after sorption test**

573

574 The replicate supernatant samples were subsequently analysed, and the results displayed in Table 4.

575 The variances here are the difference between the average data (2 values) and the difference with the

576 highest value. The variances ranges from 1 to 90% which is not unknown in biologically active

577 systems. The supernatants concentration in uranium is well below that of uranium in the seawater

578 which suggests a strong sorption.

579

580 The attempt to partition the supernatant by removing the particles with a 0.4 μm filter was
 581 unsuccessful as these samples proved vulnerable to microbial growth, as the acidification was
 582 insufficient.

583
 584 **Table 4:** Results of uranium concentration from analysis of supernatants after contact with biomass
 585 for minimum of 1 month, RSD: Standard Deviation / Mean ratio x100.
 586

Biomaterial	Test 1 ($\mu\text{g L}^{-1}$)	Test 2 ($\mu\text{g L}^{-1}$)	Mean ($\mu\text{g L}^{-1}$)	RSD (%)
Orange skin	0.038 ± 0.002	0.010 ± 0.002	0.024	57.5
Lemon skin	0.033 ± 0.002	0.040 ± 0.003	0.037	10.4
Nectarine skin	0.153 ± 0.007	0.207 ± 0.007	0.180	15.0
Grape skin	0.032 ± 0.001	0.018 ± 0.001	0.025	27.5
Grape pulp	0.019 ± 0.002	0.019 ± 0.001	0.019	1.2
Sultana whole	0.094 ± 0.003	0.006 ± 0.001	0.050	87.7
Sultana diced	0.032 ± 0.002	0.004 ± 0.001	0.018	75.5
Brussels sprouts	0.016 ± 0.001	0.016 ± 0.001	0.016	1.3
Kale diced	-	0.062 ± 0.002	0.062	-
Mange tout	0.091 ± 0.001	0.070 ± 0.003	0.080	13.5
Garlic diced	0.010 ± 0.001	0.001 ± 0.000	0.005	87.2
Peanut shell	0.017 ± 0.002	0.020 ± 0.002	0.019	7.3
Potato skin	0.017 ± 0.002	0.018 ± 0.001	0.018	3.0
Potato whole	0.009 ± 0.001	0.015 ± 0.000	0.012	22.3
Sweet potato whole	0.019 ± 0.001	0.023 ± 0.001	0.021	10.0

587

588 **4.5 ICP-MS analysis of solid material fraction after sorption test**
 589

590 The uranium content in the digested solid samples were quantified using the established calibration
 591 curve in Fig. 3, and in the majority of cases, with readings Relative Standard Deviation (RSD) below
 592 2% except for certain no-contact controls, which had readings below 5% of the lowest standard, or
 593 $0.0050 \pm 0.0005 \mu\text{g L}^{-1}$. This is over 10 times the $3\text{-}\sigma$, so can be considered to be noisy, but usable
 594 (Zhang & Davison, 1995 [57]). The digested solid sample data are reported in Table 5. Variance was
 595 also noted, as per Table 4. The range is 2%-61%. There was no correlation displayed between pair
 596 variances ($R^2=0.01$).

597

598

599 **Table 5:** Uranium content from digested solid sample analysis without (control) and with (increase)
 600 contact with seawater

Assay Sample	No contact control ($\mu\text{g kg}^{-1}$)	Test 1 Increase from control ($\mu\text{g kg}^{-1}$)	Test 2 Increase from control ($\mu\text{g kg}^{-1}$)	Average test 1&2 ($\mu\text{g kg}^{-1}$)	RSD (%)
Orange skin	0.2	336.7	131.2	234.0	43.9
Lemon skin	6.5	134.6	169.5	152.1	11.5
Nectarine skin	1.0	317.6	132.8	225.2	41.0
Grape skin	5.5	127.6	137.9	132.8	3.9
Grape pulp	5.5	42.6	10.4	26.5	60.9
Sultana whole	1.6	12.2	16.8	14.5	16.0
Sultana diced	1.6	12.2	16.8	18.2	3.7
Brussels sprouts	0.0	15.6	13.4	14.5	7.4
Kale diced	6.5	-	205.6	205.6	-
Mange tout	2.3	43.8	40.8	42.3	3.7
Garlic diced	1.1	81.4	20.8	51.1	59.3
Peanut shell	57.8	68.2	153.9	111.0	38.6
Potato skin	54.3	199.4	419.5	309.4	35.6
Potato whole	0.3	10.3	11.2	10.8	4.0
Sweet potato whole	1.5	18.6	18.0	18.3	1.6

601

602

603 The sweet potato skin samples, and the Brussels sprout controls suffered a fungal attack, and could
 604 not be analysed by ICP-MS. Kale diced 1 was lost during an accident during digestion, so could not
 605 be completed.

606

607 The loading of U on the biomass samples was then analysed. Data recorded either after 2 months
608 (week beginning 23 Jan 19 - week beginning 11 March 19) contact time or 1 month (week 17 June
609 19 – week beginning 22 July 19) re-plotted in Fig.4 as average fractions of U absorbed per mass unit
610 of biomass.

611

612 **Fig. 3:** Average amount of U absorbed per dry mass unit of biomass

613

614

615 The highest sorption by weight was by the potato skin ($255 \mu\text{g kg}^{-1}$), then by orange peel ($233 \mu\text{g kg}^{-1}$)
616 and by nectarine peel ($224 \mu\text{g kg}^{-1}$). In addition kale diced performed significantly better in this
617 metric than the others ($209 \mu\text{g kg}^{-1}$).

618

619 Peanut shells get a special mention as they had the third highest actual U content measured of any of
620 the samples, but the material efficiency was low, due to high background U concentration in the
621 control, and high density of the material. In contrast, potato skin actual U was not significantly
622 different from other materials in measured concentration, but its low density made it appears the
623 greatest. Further testing is required to establish if the high capture concentration represents an efficient
624 surface, or an artefact of the high surface to mass ratio of the material.

625

626 Considering the U fraction between the solid phase and its total amount (consisting of the U sorbed
627 onto suspended solids and the U in the aqueous phase) it is clear that the fractionation by the grapes
628 (97%, except pulped sultanas, which would, if one replicate was discounted) are most effective in
629 retaining the U, followed by garlic (96%), Brussels sprouts (94%), then the orange peel (93%).

630 Kale diced and Peanut shells also had good capture rates (90%). Full data are presented in Fig. 5.

631
632 **Fig. 5:** Average mass fractions (Eq. 1) of U absorbed on the bio-solids

633
634 However, the general level of capture seems to indicate that the surfaces were strongly depleting the
635 U from the liquid phase, and that the net capture is unlikely to represent saturation of the surfaces.

636
637 The fraction ratio does indicate that the mange tout was not effective. This is a likely indicator that
638 the antioxidants, such as retinoic acid was not providing an effective agent in reduction, despite it
639 being known to function as such in other contexts, likely due to conditions in the sample vials.

640
641 Despite the high concentration on the surface of the potato skin and nectarine peel by weight, the net
642 captures for these materials are weaker against the majority. Further testing is needed to establish if
643 the capture % was impacted due to saturation, or if this is indicative of low retention due to decay.

644
645 The sorption coefficients K_d were calculated using Eq. 2. Details are given in Table 6. Data reported
646 in Table 6 show that the K_d values are ranging from 52 to 1866 mL g⁻¹. As displayed in Fig. 5, it is
647 unlikely that these are a true equilibrium value, so should be considered indicative rather than a formal
648 measurement. The highest indicative K_d was by the garlic (1886 L kg⁻¹), then by orange peel (1669.5
649 L kg⁻¹) and by nectarine peel (1401 L kg⁻¹).

650
651 Stronger sorption's are presumed to be due to uranyl reduction in tetravalent uranium by the
652 antioxidants associated to these biomaterials. It was also suggested that the chemical sorption
653 reactions may be coupled with colloidal aggregation, suggesting irreversible sorption hence
654 increasing K_d values.

Sample	S. 1: U concentration on biomass ($\mu\text{g kg}^{-1}$)	S 1. U concentration in fluid phase ($\mu\text{g L}^{-1}$)	S 1. K_d (mL g^{-1})	S 2. U concentration on biomass ($\mu\text{g kg}^{-1}$)	S 2. U concentration in fluid phase ($\mu\text{g L}^{-1}$)	S 2. K_d (mL g^{-1})	Average K_d (mL g^{-1})	SD (mL g^{-1})	RSD (%)
Orange Skin	336.75	0.246	1370.8	131.17	0.067	1968.2	1669.5	298.7	17.9
Lemon Skin	134.58	0.214	630.0	169.53	0.261	649.9	640.0	9.9	1.6
Nectarine Skin	317.61	1.019	311.7	132.76	1.333	99.6	205.6	106.1	51.6
Grape Skin	127.64	0.210	607.0	137.88	0.121	1142.7	874.8	267.9	30.6
Grape Pulp	42.61	0.122	348.7	10.36	0.121	85.3	217.0	131.7	60.7
Sultanas Diced	12.19	0.610	20.0	16.83	0.040	418.4	219.2	199.2	90.9
Sultanas Pulped	17.50	0.208	84.1	18.85	0.029	644.6	364.4	280.2	76.9
Brussels Sprouts Diced	15.56	0.105	148.6	13.42	0.102	131.8	140.2	8.4	6.0
Kale Diced	-	-	-	212.10	0.405	524.0	524.0	-	-
Mange Tout	43.84	0.950	46.1	40.75	0.694	58.7	52.4	6.3	12.0
Garlic Diced	81.41	0.105	772.8	20.79	0.007	2960.6	1866.7	1093.9	58.6
Peanuts Shell	68.18	0.195	349.9	153.91	0.236	653.0	501.5	151.5	30.2
Potato Skin	199.40	0.195	1023.4	419.47	0.236	1779.6	1401.5	378.1	27.0
Potato Diced	10.33	0.077	133.8	11.20	0.131	85.5	109.6	24.2	22.0
Sweet Potato Diced	18.63	0.172	108.2	18.04	0.213	84.8	96.5	11.7	12.1

655 **Table 6:** Sorption coefficients (K_d) of samples.656
657
658

659
660 **Fig. 6:** K_d values as estimated for the sorption of uranium on biomaterials.

661
662
663
664

665 **5 Discussion**

666

667 Based on the sorption results presented in Section 4 an initial picture emerges.

668 This initial picture may be seen as faded by the dispersion of the experimental sorption data gained in
669 the former section. This is due to the bio-variability of the samples which yield composition changes
670 of the biomass samples. This is the fruit of plant growing state due to soil plant interaction, watering
671 conditions, plant/fruit orientation, maturity grade (leave, fruit, tuber ...), sample preparation including
672 sample cutting, size of biomass phases and biofouling. These factors may affect element uptake or
673 K_d by a factor 2.

674 It is noticeable that the samples with the highest retention all are associated with materials known to
675 release free aromatic chemicals into solution. Grape fermentation is known, driven by their high sugar
676 content, but garlic, Brussels sprouts and kale all be composed of and release free aromatic chemicals
677 such as polyphenols into solution. This would be an example of a suitable material for a contained
678 source/collector system.

679

680 However the greatest proportion of polyphenols and antioxidants are currently bound with insoluble
681 polymers and some of them (dry weighted, dw) sorb strongly uranyl ion, their polyphenols (PP)
682 content is high.

683

684 Grapes are found with 40 to 400 mg PP per 100 g dw (Nile, *et al*, 2013 [58]; Pastrana-Bonilla, *et al*,
685 2003 [59]). Garlic is found with 40 to 50 mg PP per 100 g dw (Chekki, *et al*, 2014 [60]). Brussels
686 sprouts may contain about 100 mg PP per 100 g dw (Cieslik, *et al.*, 2006 [61]). Kale diced samples

687 have 500 to 600 mg PP per 100 g dw (Sikora & Bodziarczyk, 2012 [62]). Peanut shells are found with
688 300 to 450 mg PP per 100 g dw (Rosales-Martínez, *et al.*, 2014 [63]; Qiu, *et al.*, 2012 [64]). Orange
689 skins have 300 to 450 mg PP per 100 g dw (Abd El-aal & Halaweish, 2010 [65]). Lime skins are
690 found with about 60 mg PP per 100 g dw (Safdar, *et al.*, 2017 [66]). Potato skins have 10 to 35 mg
691 PP per 100 g dw (Akyol, *et al.*, 2016 [67]). Nectarine skins are found with 20 to 60 mg PP per 100 g
692 dw (Gil, *et al.*, 2002 [68]), and mange tout samples are found with about 10 mg PP per 100 g dw
693 (Lanzmann-Petithory, 2002 [69]). These polyphenols are expected to increase sorption. A plot of K_d
694 versus the PP concentration displays a correlation (see Fig. 7)]. There are several reasons why a
695 dispersion of data is observed. Some of the compounds which are included in the PP fraction, are
696 soluble while others remains in the biomaterial. This may also be due to the size or the fractal aspect
697 of the biomass phases. Alternatively, their reported PP concentrations are not fully reflective of the
698 natural variability between specimens. Most critically, we must also consider if part of the sorption is
699 irreversible, which will disproportionately impact the ratio. And this may be the case since samples
700 post contact show presence of aggregates (see Section 4.1) that eventually makes the sorption
701 irreversible even more makes the leaching more difficult as observed or the long contact time samples.

702

703

704 **Fig. 7:** Plot of K_d with polyphenol (PP) concentration (biomass dry weight: dw).

705

706

707 In addition to the PP themselves, there are other released compounds, which may impact the sorption
708 rates. Grape fermentation is well known for its alcohol production driven by their high sugar content,
709 but garlic, Brussels sprouts and kale all release various organo-sulphur compounds such as allicin

710 from garlic, glucosinolate from Brussels sprouts and kale, while peanut shells release compounds
711 such as luteolin quickly under mildly anaerobic conditions e.g. Eksi, *et al.*, (2019) [70]. While
712 samples were not sealed air tight, it suggests these localised low oxygen conditions within the samples
713 are promoting depositions, which was detectable while working with the samples. These processes
714 are commonly supposed to be microbe-associated; it will consequently be important to test their
715 effects, and ensure controls are adequate to prevent leakage to environment.

716

717 The data also suggests two potential scenarios: materials with sacrificial antioxidants are more
718 effective in retention, compared with more locational-specific antioxidants, or these materials are
719 emitting chemicals which are stimulating the microcosm, which encourages deposition. These are not
720 mutually exclusive hypotheses, but it is likely that one will have greater influence. In addition, it will
721 dictate some of the practicalities of interaction. If the process requires release to solution, a contact
722 space over the materials is required, while a surface micro-organism paradigm can be more enclosed.

723

724 The failure of the supernatant partitioning, and the loss of several of the samples through post work
725 growth shows how biologically active these samples can be, even downstream from the sample itself,
726 and that the controls in place were insufficient. These lessons were incorporated in the updated
727 experimental design, through post extraction controls, and with the inclusion of containing structures,
728 specifically filter bags.

729

730 In terms of feasibility, the work discussed above has demonstrated that while using biomass, capture
731 of U from seawater is possible, further work is needed to increase the usability of the methodology.
732 The small sample batches are limited in capacity, and which has acted as a threshold on the quantities

733 sorbed over time, as the low total system capacity is only of the order of 0.1-0.2 μg , and with most of
734 the samples were in the 80-95% capture range suggesting this actually might represent a systemic
735 limit rather than a true equilibrium. Therefore, reducing the solid to seawater ratios are important,
736 which can be achieved with smaller solid sample and larger seawater volumes, and larger vessels, to
737 increase the water fraction.

738

739 In saline surface water, uranium is conventionally considered to be hexavalent, which, under neutral
740 conditions, undergoes strong but reversible sorption. When reduced, for example by the antioxidant-
741 functional groups on the biomass materials, to tetravalent uranium which exhibits stronger sorption.
742 This is commonly supposed to be due to a Coulomb effect making the binding of U^{4+} complexes
743 stronger than for the UO_2^{2+} complexes. Therefore, a reducing agent such as antioxidants from the
744 biomass material, introduced into solution, increase the proportion of U^{4+} present, and higher K_d
745 values for uranium. Finally, presence of fine biomass material facilitates condensation of the colloids
746 via aggregation, masking metal ions and complexes in the biomaterial. This behaviour makes the
747 sorption irreversible with the embedding of the metal in the colloidal structure.

748

749 Additionally, these materials had undergone no modification, beyond the sizing process: for example,
750 to establish the synthetic materials, they are pre-treated with acid to prepare sorption sites for
751 exchange. This process could also benefit the materials. There is also the question of whether
752 materials currently being evaluated could be used in conjunction. For example, would combining the
753 kale's retention chemicals with the potato skin's surface area be a potential path to improved
754 performance? These questions indicate that while there are significant improvements necessary to
755 increase the method to practicality, there are pathways to explore for improved efficiency.

756

757 The bio material studied is cheaper than the low cost material itself (fruit, green vegetable and tuber
758 samples) because it consists of peals, fragments or rests (bio-waste). The only costs associated to
759 their use are: their size reduction, drying, transport, package/bag setting and dipping in seawater.
760 The high costs associated to product synthesis are avoided. Actually, full cost analysis e.g. in \$ or J
761 (for EROEI approach) is foreseen in a separate study.

762

763 Based on the sorption results, garlic, grape skin, orange skin, potato skin and kale are all prioritized
764 for further study. The fact that all of these exhibit high surface to mass materials should be noted, and
765 future work will aim to produce samples that are more consistent in particle size, and other materials
766 with similar properties are targeted for future work. Reducing the particle size will also improve
767 general efficiency.

768

769

770 **6 Conclusion**

771

772 This work has established that the concept of utilizing the selected low cost materials to concentrate
773 the low U content of seawater is feasible, but there are many challenges ahead in developing this
774 technology to practicality. Furthermore, the design for comprehensive experimental methodology will
775 look like, has been sorted out for further investigations.

776

777 Sorption tests carried out for a minimum of 1 month in natural saline water from the Irish Sea revealed
778 sorption of uranium from seawater onto the following material.

779 Data reported in sorption capacity ($\mu\text{g kg}^{-1}$) show the average increase in uranium content for
780 potato whole ($10.44 \mu\text{g L}^{-1}$), Sultanas whole ($12.93 \mu\text{g L}^{-1}$), Brussels sprouts ($14.49 \mu\text{g L}^{-1}$), to
781 nectarine skin ($224.16 \mu\text{g L}^{-1}$), orange skin ($233.76 \mu\text{g L}^{-1}$) and potato skin ($255.16 \mu\text{g L}^{-1}$). Sorption
782 data expressed in fraction (%) of sorbed U increased according to nectarine skin (53.2%), mange tout
783 (53.9%), potato skin (83.6%), up to grape pulp (96.9%), grape skin (97.0%) and Sultanas diced
784 (97.0%).

785

786 Sorption coefficient (K_d) values were found ranging from $\sim 50 \text{ mL g}^{-1}$ (mange tout, sweet potato dices)
787 to $\sim 2000 \text{ mL g}^{-1}$ (Orange skin, Garlic dices). Polyphenol (PP) rich biomass samples are expected to
788 increase sorption. A plot of K_d with the PP concentration displays a correlation. Stronger sorptions
789 are presumed to be due to uranyl reduction in tetravalent uranium by the antioxidants found onto these
790 biomaterials. Since K_d values are of the order of $50\text{-}2000 \text{ mL g}^{-1}$, it was also suggested that the
791 chemical sorption reactions may be associated with colloidal aggregation, suggesting irreversible
792 sorption. This screening study was aimed to allow selection of specific bio-waste material absorbents
793 to be tested in detail.

794

795 Based on the sorption results, garlic, grape skin, orange skin, potato skin and kale are prioritized for
796 further study.

797

798

799 **Acknowledgements**

800 The work is part of the program: *Nuclear as a Renewable*. It is also part of a PhD work carried out in
801 the frame of the Centre of Doctoral Training managed at Lancaster University by Professor Colin

802 Boxall. Acknowledgements are due to Dr Richard Wilbraham for the FTIR record of the samples, Dr
803 Farid Aiouache for his interest in this work and Dr Jackie Pates for delivering the uranium standard.
804 The work, supported partially by the New Generation Nuclear program sponsored by EPSRC, was
805 carried in the Engineering Department and at the Lancaster Environmental Centre of The Lancaster
806 University.

807

808 **CReDiT**

809 Author contributions to the published work:

- 810 • **Claude Degueldre:** Conceptualization, Methodology, Supervision Reviewing and
811 Management.
- 812 • **Hao Zhang:** Data curation, Software, Validation, Writing. Visualization.
- 813 • **Steven McGowan:** Investigation, Batch Preparation, Measurements, Writing - Original Draft.

814

815

816

817 **References**

-
- [1] F. Birol, Nuclear Power in a clean energy system. *Fuel Report*, IEA, May (2019) [.https://www.iea.org/reports/nuclear-power-in-a-clean-energy-system](https://www.iea.org/reports/nuclear-power-in-a-clean-energy-system)
- [2] C. Degueldre, H.J. Ulrich, H. Silby, Sorption of ²⁴¹Am onto montmorillonite, illite and hematite colloids. *Radiochim. Acta*, 1994, 65, 173-179. <https://doi.org/10.1524/ract.1994.65.3.173>
- [3] C. Degueldre, H.-R. Pfeiffer, W. Alexander, B.Wernli, R. Bruetsch . Colloid properties in granitic groundwater systems. I: Sampling and characterisation. *Appl. Geochem.*, 1996, 11, 677-695. [https://doi.org/10.1016/S0883-2927\(96\)00036-4](https://doi.org/10.1016/S0883-2927(96)00036-4)
- [4] T. H. Pigford, Environmental aspects of nuclear energy production. *Annual Rev. Energy*, 1976 ,1, 515-559. <https://doi.org/10.1146/annurev.ns.24.120174.002503>.
- [5] R. C. Ewing, Environmental impact of the nuclear fuel cycle. *Geological Soc., London, Special Publications*, 2004, 236, 7-23. <https://doi.org/10.1144/GSL.SP.2004.236.01.02>
- [6] NEA and IAEA, Uranium 2016 – resource, production and demand. *OECD publishing*, (2016) 548. <https://doi.org/10.1787/uranium-2016-en>
- [7] C. A. Degueldre, R. J Dawson, V. Najdanovic-Visak. Nuclear fuel cycle, with a liquid ore and fuel: toward renewable energy. *Sustainable Energy & Fuels*, 2019, 3, 1693-1700. <https://doi.org/10.1039/C8SE00610E>
- [8] B.-M. Jun, H.-K. Lee, S. Park, T.-J. Kim, Purification of uranium-contaminated radioactive water by adsorption: A review on adsorbent materials, *Separation and Purification Technology*, 2022, 278, 119675. <https://doi.org/10.1016/j.seppur.2021.119675>
- [9] T. Sugo, M. Tamada, T. Seguchi, T. Shimizu, M. Uotani, R. Kashima. Recovery System for Uranium from Seawater with Fibrous Adsorbent and Its Preliminary Cost Estimation. *J. Atom. Energy Soc. Japan*, 2001,43, 1010-1016. <https://doi.org/10.1039/C4TA06120A>
- [10] E. Schneider, D. Sachde, The Cost of Recovering Uranium from Seawater by a Braided Polymer Adsorbent System. *Sci. Global Security*, 2012, 21, 134-163.
- [11] A. Dong, T. Dai, M. Ren, X. Zhao, S. Zhao, Y. Yuan, Q. Chen, N. Wang, Functionalization and Fabrication of Soluble Polymers of Intrinsic Microporosity for CO₂ Transformation and Uranium Extraction, *Engineered Science*, 2019, 5, 56-65, [DOI:10.30919/es8d613](https://doi.org/10.1016/j.es8d613)
- [12] A. Dong, Y. Zhu, M. Ren, X. Sun, V. Murugadoss, Y. Yuan, J. Wen, X. Wang, Q. Chen, Zh. Guo, N. Wang, Remarkably Enhanced CO₂ Uptake and Uranium Extraction by Functionalization of Cyano-bearing Conjugated Porous Polycarbazoles, *Engineered Science*, 2019, 6, 44-52, [DOI:10.30919/esee8c217](https://doi.org/10.1016/j.esee8c217)
- [13] H. Liu, Y. Mao, Graphene Oxide-]based Nanomaterials for Uranium Adsorptive Uptake, *ES Materials & Manufacturing*, 2021, 13, 3-22, <https://dx.doi.org/10.30919/esmm5f453>

- [14] H. Wei, J. Ma, Y. Shi, D. Cui, M. Liu, N. Lu, N. Wang, T. Wu, E. K. Wujcik, Z. Guo, Sustainable Cross-linked Porous Corn Starch Adsorbents with High Methyl Violet Adsorption, *ES Materials & Manufacturing*, 2018, 2, 28-34,
- [15] J. Song, Y. Wang, J. Qiu, High Adsorption Performance of Methyl Blue from Aqueous Solution using Hyper-branched Polyethyleneimine Grafted MWCNTs as an Adsorbent, *ES Materials & Manufacturing*, 2019, 3, 29-37,
- [16] J. Chen, X. Wang, Y. Huang, S. Lv, X. Cao, J. Yun, D. Cao, Adsorption removal of pollutant dyes in wastewater by nitrogen-doped porous carbons derived from natural leaves, *Engineered Science*, 2019, 5, 30-38, DOI:10.30919/es8d666
- [17] C. Lin, Z. Qiao, J. Zhang, J. Tang, Z. Zhang, Z. Guo, Highly Efficient Fluoride Adsorption in Domestic Water with RGO/Ag Nanomaterials, *ES Energy & Environment*, 2019, 4, 27-33, DOI:10.30919/esee8c217
- [18] Y. Wang, W. Xie, H. Liu, H. Gu, Hyperelastic magnetic reduced graphene oxide three-dimensional framework with superb oil and organic solvent adsorption capability, *Adv. Compos. Hybrid Mater.* 2020, 3, 473-484. <https://doi.org/10.1007/s42114-020-00191-z>
- [19] X. Shi, J. Hong, C. Wang, S. Kong, J. Li, D. Pan, J. Lin, Q. Jiang, Z. Guo, Preparation of Mg,N-co-doped lignin adsorbents for enhanced selectivity and high adsorption capacity of As (V) from wastewater, *Particuology*, 2021, 58, 206-213, <https://doi.org/10.1016/j.colsurfa.2021.127279>
- [20] J. Hong, L. Kang, X. Shi, R. Wei, X. Mai, D. Pan, N. Naik, Z. Guo, (2022) Highly efficient removal of trace lead (II) from wastewater by 1,4-dicarboxybenzene modified Fe/Co metal organic nanosheets, *J. Mater. Sci. Technol.*, 2022; 98, 212-218, <https://doi.org/10.1016/j.jmst.2021.05.021>
- [21] Y. N. Mata, M. L. Gallego Blázquez, A. Ballester, F Gonzalez, J. A. Muñoz. Sugar-beet pulp pectin gels as biosorbent for heavy metals: Preparation and determination of biosorption and desorption characteristics. *Chem. Eng. J.*, 2009, 150, 289-301. <https://doi.org/10.1016/j.cej.2009.01.001>
- [22] W.C.Li, H.F.Tse, L.Fok, Plastic waste in the marine environment: A review of sources, occurrence and effects, *Science of The Total Environment*, 566–567 (2016) 333-349 <https://doi.org/10.1016/j.scitotenv.2016.05.084>
- [23] J. Park, G. A. Gill, J. E. Strivens, L. Kuo, R. T. Jeters, A. Avila, G. T. Bonheyo, Effect of Biofouling on the Performance of Amidoxime-Based Polymeric Uranium Adsorbents. *Ind. Eng. Chem. Res.*, 55 (2016) 4328-4338. <https://doi.org/10.1021/acs.iecr.5b03457>
- [24] A. Nakajima, T. Horikoshi, T. Sakaguchi, Recovery of uranium by immobilized microorganisms. *Eur. J. Appl. Microbiol. Biotechnol.*, 16 (1982) 88-91. <https://doi.org/10.1007/BF00500732>
- [25] S. Ramamoorthy, A. Raghavan, M. Santappa. Complexes of uranyl ion with butyric and isobutyric acids. *J. Inorg. Nucl. Chem.*, 31 (1969) 1765-1769. [https://doi.org/10.1016/0022-1902\(69\)80394-5](https://doi.org/10.1016/0022-1902(69)80394-5)
- [26] E. El-Sheikh. Application of waste frying oil as an extractant for uranium from sulfate leach liquor. *J. Radiation Res. Appl. Sci.*, 9 (2016) 155-163. <https://doi.org/10.1016/j.jrras.2015.10.003>

- [27] G. Tang, W.M. Wu, D.B. Watson, J.C. Parker, C.W. Schadt, X.Q. Shi, S.C. Brooks, U(VI) Bioreduction with Emulsified Vegetable Oil as the Electron Donor – Model Application to a Field Test. *Environm. Sci. Technology*, 47 (2013) 3218-3225. <https://doi.org/10.1021/es304643h>
- [28] M.S. Diallo, M. R. Kotte, M. Cho. Mining Critical Metals and Elements from Seawater: Opportunities and Challenges. *Environ. Sci. Technol.*, 49 (2015) 9390-9399. <https://doi.org/10.1021/acs.est.5b00463>
- [29] S. Gondhalekar, S. Shukla. Equilibrium and kinetics study of uranium(VI) from aqueous solution by Citrus limetta peels. *J. Radioanal. Nucl. Chem.*, Issue 302 (2014) 451–457. <https://doi.org/10.1007/s10967-014-3165-3>
- [30] B. Satari, K. Karimi. Citrus processing wastes: Environmental impacts, recent advances, and future perspectives in total valorization. *Resources, Conservation and Recycling*, 129 (2018) 153-167. <https://doi.org/10.1016/j.resconrec.2017.10.032>
- [31] A. Nakajima, T. Sakaguchi, Adsorption of Uranium by Vegetable Crude Drugs. *Agricultural and Biological Chem.*, 53 (1989) 2853-2859. <https://doi.org/10.1271/bbb1961.53.2853>
- [20] Z. Aly, V. Luca, Uranium extraction from aqueous solution using dried. *J Radioanal. Nucl. Chem.*, 295 (2013) 889-900. <https://doi.org/10.1007/s10967-012-1851-6>
- [33] H. N. Bhatti, S. Hamid, Removal of uranium(VI) from aqueous solutions using *Eucalyptus citriodora* distillation sludge, *International Journal of Environmental Science and Technology* 11 (2014) 813–822. <https://doi.org/10.1007/s13762-013-0267-3>
- [34] P. D. Pathak, S. A. Mandavgane, B. D. Kulkarni. Fruit peel waste as a novel low-cost bio adsorbent. *Rev. Chem. Eng.*, 31 (2015) 361-381. <https://doi.org/10.1515/revce-2014-0041>
- [35] T. Sakaguchi, A. Nakajima, T. Horikoshi. Absorption of uranium from sea water by biological substances. *Nippon Nogei Kagaku Kaisi*, 53 (1979) 149-156.
- [36] T. Sakaguchi, T. Horikoshi, A. Nakajima. Adsorption of Uranium by Chitin Phosphate and Chitosan Phosphate. *Agricultural and Biological Chem.*, 10 (1981) 2191-2195.
- [37] S. Xie, X. Zhang, M. P. Walcott, H. Lin, Applications of Cellulose Nanocrystals: A Review, *Engineered Science*, 2018, 2, 4-16,
- [38] J. Cai, W. Xu, Y. Liu, Z. Zhu, G. Liu, W. Ding, G. Wang, H. Wang, Y. Luo Robust Construction of Flexible Bacterial Cellulose@Ni(OH)₂ paper: Toward High Capacitance and Sensitive H₂O₂ Detection, *Engineered Science*, 2019, 5, 21-29,
- [39] B. Yuan, L. Li, V. Murugadoss, S. Vupputuri, J. Wang, N. Alikhani, Z. Guo, Nanocellulose-based composite materials for wastewater treatment and waste-oil remediation, *ES Food & Agroforestry*, 2020, 1, 41-52,
- [40] B. O. Boni, L. Lamboni, B. M. Bakadia, S. A. Hussein, G. JYang, Combining Silk Sericin and Surface Micropatterns in Bacterial Cellulose Dressings to Control Fibrosis and Enhance Wound Healing, *Engineered Science*, 2020, 10, 68-77,

-
- [41] L. Mu, Y. Dong, L. Li, X. Gu, Y. Shi, Achieving High Value Utilization of Bio-oil from Lignin Targeting for Advanced Lubrication, *ES Materials & Manufacturing*, 2021, 11, 72-80
- [42] C. Joseph, L. R. Van Loon, A. Jakob, R. Steudtner, K. Schmeide, S. Sacks, G. Bernhard. Diffusion of U(VI) in Opalinus Clay: Influence of temperature and humic acid, *Geochim. Cosmochim. Acta*, 109 (2013) 74-89. <https://doi.org/10.1016/j.gca.2013.01.027>
- [43] C. Degueldre, A. Bilewicz, W. Hummel, J. L. Loizeau. Sorption behaviour of Am on marl groundwater colloids. *J. Environm. Radioactivity*, 55 (2001) 241-255. <https://doi.org/10.1016/10.1021/es00072a012>
- [44] B. McKee, J. Todd. Uranium behavior in a permanently anoxic Fjord: Microbial control? *Limnology and Oceanography*, 38 (1993) 408-414. <https://doi.org/10.4319/LO.1993.38.2.0408>
- [45] A. Boudet. Lignins and lignification: Selected issues. *Plant Physiology and Biochem.*, 38 (2000) 81-96. [https://doi.org/10.1016/S0981-9428\(00\)00166-2](https://doi.org/10.1016/S0981-9428(00)00166-2)
- [46] L. Zhang, R. Liu, B.W. Gung, S. Tindall, J.M. Gonzalez, J.J. Halvorson, A.E. Hagerman. Polyphenol–Aluminium Complex Formation: Implications for Aluminium Tolerance in Plants. *J. Agric. Food Chem*, 64 (2016) 3025-3033. <https://doi.org/10.1021/acs.jafc.6b00331>
- [47] K. Jones. A comparison of the distribution of heterotrophic nitrogen fixing bacteria in coastal waters of Morecambe Bay, UK, the Ligurian Sea, France, the Bay of Naples, Italy and the Pacific Ocean, Hawaii, USA; in *Estuaries and Coasts: Spatial and Temporal intercomparison*. Eds M. Elliott and J.P. Ducrotoy, ESCA19, Symposium, University of Caen, Publish. Olsen & Olsen (1991). <https://doi.org/10.1006/jmsc.1996.0115>
- [48] C. Degueldre. *The analysis of nuclear materials and their environments*, Springer, (2017) pp. 288. <https://doi.org/10.1007/978-3-319-58006-7>
- [49] R.W. Laane, A. J. Southward, D. J. Slinn, J. Allen, G. Groeneveld, A. Vries, Changes and causes of variability in salinity and dissolved inorganic phosphate in the Irish Sea, English Channel, and Dutch coastal zone. *ICES J. Marine Sci.*, 53 (1996) 933–944. <https://doi.org/10.1006/jmsc.1996.0115>
- [50] M. Beazley, R. Martinez, P. Sobczyk, S. Webb, M. Taillefert. Uranium biomineralization as a result of bacterial phosphatase activity: insights from bacterial isolates from a contaminated subsurface. *Environ. Sci. Technol.*, 41 (2007) 5701-5707. <https://doi.org/10.1021/es070567g>
- [51] A. Gregorič, J. Kotnik, M. Horvat, N. Pirrone. Dissolved radon and gaseous mercury in the Mediterranean seawater, *J. Environm. Radioactivity*, 99 (2008) 1068-1074. <https://doi.org/10.1016/j.jenvrad.2007.12.023>
- [52] M. Walker, K. Rose. The radioactivity of the sea. *Nucl. Energy*, 29 (1990) 267-278.
- [53] D. Gardner. *Marine Pollution: Diagnosis and therapy*. Springer (1973).
- [54] D. J. Assinder. A review of the occurrence and behaviour of neptunium in the Irish Sea, *J. Environm. Radioactivity*, 44 (1999) 335-347. [https://doi.org/10.1016/S0265-931X\(98\)00139-8](https://doi.org/10.1016/S0265-931X(98)00139-8)

[55] C. Turetta, G. Cozzi, A. Varga, P. Cescon. Platinum group elements determination in seawater by ICP-SFMS: initial results, *J. de Physique* 107 (2003) 1-4. <https://doi.org/10.1051/jp4:20020544>

[56] E. D. Goldberg, V. Hodge, P. Kay, M. Stallard, M. Koide. Some comparative marine chemistries of platinum and iridium. *Appl. Geochem.*, 1 (1986) 227-232. [https://doi.org/10.1016/0883-2927\(86\)90092-2](https://doi.org/10.1016/0883-2927(86)90092-2)

[57] H. Zhang, W. Davison. Performance characteristics of diffusion gradients in thin films for the in situ measurement of trace metals in aqueous solution. *Anal. Chem.*, 67 (1995) 3391-3400. <https://doi.org/10.1021/ac00115a005>

[58] S. H. Nile, S. H. Kim, Eun Young Ko, Se Won Park. Polyphenolic Contents and Antioxidant Properties of Different Grape (*V. vinifera*, *V. labrusca*, and *V. hybrid*) Cultivars. *BioMed. Research International*, 2013 (2013) 1-5. <https://doi.org/10.1155/2013/718065>

[59] C. C. A Pastrana-Bonilla, S. Sellappan, G. Krewer. Phenolic Content and Antioxidant Capacity of Muscadine Grapes. *J. Agric. Food Chem.*, 51 (2003) 5497-5503. <https://doi.org/10.1021/cf030113c>

[42] R.Z. Chekki, A. Snoussi, I. Hamrouni, N. Bouzouita N. Chemical composition, antibacterial and antioxidant activities of Tunisian garlic (*Allium sativum*) essential oil and ethanol extract, *Mediterranean J. Chem.*, 3 (2014) 947-956. <https://doi.org/10.13171/mjc.3.4.2014.09.07.11>

[61] E. Cieslik, A. Greda, W. Adamus. Contents of polyphenols in fruit and vegetables. *Food Chem.*, 94 (2006) 135-142. <https://doi.org/10.1016/j.foodchem.2004.11.015>

[62] E. Sikora, I. Bodziarczyk. Composition and Antioxidant Activity of Kale (*Brassica Oleracea* L. Var. *Acephala*) Raw and Cooked. *Acta Sci. Pol. Technol. Aliment Actions*, 11 (2012) 239-248. PMID: 22744944

[63] P. Rosales-Martínez, S. Arellano-Cárdenas, L. Dorantes-Álvarez, F. García-Ochoa, M. del S. López-Cortez. Comparison Between Antioxidant Activities of Phenolic Extracts from Mexican Peanuts, Peanuts Skins, Nuts and Pistachios, *J. Mex. Chem. Soc.*, 58 (2014) 185-193. ISSN 1870-249X

[64] J. Qiu, L. Chen, Q. Zhu, D. Wang, W. Wang, X. Sun, X. Liu. Screening natural antioxidants in peanut shell using DPPH–HPLC–DAD–TOF/MS methods. *Food Chemistry*, 135 (2012) 2366-2371. <https://doi.org/10.1016/j.foodchem.2012.07.042>

[65] H. Abd El-aal, F. Halaweish. Food preservative activity of phenolic compounds in orange peel extracts (*Citrus Sinensis* L.). *Lucrări Științifice*, 53 (2010) 457-464

[66] M.N. Safdar, T. Kausar, S. Jabbar, A. Mumtaz, K. Ahad, A.A. Saddozai. Extraction and quantification of polyphenols from kinnow (*Citrus reticulata* L.) peel using ultrasound and maceration techniques, *J. Food Drug Anal.*, 25 (2017) 488-500. <https://doi.org/10.1016/j.jfda.2016.07.010>

[67] H. Akyol, Y. Riciputi, E. Capanoglu, M. Fiorenza Caboni, V. Verardo. Phenolic Compounds in the Potato and Its Byproducts: An Overview. *Int. J. Mol. Sci.*, 17 (2016) 835. <https://doi.org/10.3390/ijms17060835>

[68] M.I. Gil, F.A. Tomás-Barberán, B. Hess-Pierce, A.A. Kader. Antioxidant Capacities, Phenolic Compounds, Carotenoids, and Vitamin C Contents of Nectarine, Peach, and Plum Cultivars from California. *J. Agric. Food Chem.*, 50 (2002) 4976–4982. <https://doi.org/10.1021/jf020136b>

[69] D. Lanzmann-Petithory, *La diététique de la longévité*. Ed. Odile Jacob, Paris 2002. ISBN-978-27381-8538-9

[70] G. Eksi, S. Kurbanoglu, S. Ozkan. Fortification of Functional and Medicinal Beverages With Botanical Products and Their Analysis. Chapt. 12.2.2 Organo-Sulfur Compounds, in *Engineering Tools in the Beverage Industry* (2019). <https://doi.org/10.1016/B978-0-12-815258-4.00012-3>